Simulating the performance of the Southern Wide-view Gamma-ray Observatory

H. Schoorlemmer,^{a,*} **R. Conceição**^{b} **and A. J. Smith**^{c} **on behalf of the SWGO Collaboration**
(a complete list of authors can be found at the end of the proceedings)

^{a}*Max-Planck-Institut für Kernphysik, Saupfercheckweg 1, Heidelberg, Germany*

^{b}*LIP/IST, Lisboa, Portugal*

^{c}*Department of Physics, University of Maryland, College Park, MD, USA*

 E-mail: harmscho@mpi-hd.mpg.de

The Southern Wide-view Gamma-ray Observatory (SWGO) will be a next-generation gamma-ray observatory using a large array of particle detectors at a high elevation site in South America. This project is currently in a three years R&D phase in which the design will be optimised for cost and performance. Therefore it is crucial to efficiently evaluate the impact of different design options on the scientific objectives of the observatory. In this contribution, we will introduce the strategy and the simulation framework in which this evaluation takes place.

---

*Presenter

1. Context

The Southern Wide-field Gamma-ray Observatory[1] will be a cosmic particle observatory to be constructed at a high-elevation site (> 4.4 km above sea-level) in the Andes mountain range. Currently this project is in a Research and Development (R&D) phase, which is expected to be concluded in 2023 with a final design for the observatory. To deal with the various aspects of the R&D phase the collaboration generated five working groups with different tasks:

- *science* – evaluation and development of the science cases,

- *analysis and simulation* – estimation of the performance of different design options,

- *detector* – assessment of the hardware design,

- *site* – characterisation of the several possible site locations,

- *outreach and communication* – preparation of internal and external communication materials.

These working groups organise themselves with regular, typically bi-weekly, calls and the communication between working groups is guaranteed by monthly calls between the working group coordinators and two collaboration meetings per year. In this contribution the strategy to optimise the detector design of the *analysis and simulation* working group is presented.

2. Simulation Chain

The objective is to evaluate the performance of several design choices in order to optimise the final design. To get a fair comparison between the different component and layout options, all design options will be performed in a single framework. It was decided to adapt and expand the simulation and reconstruction framework of the HAWC collaboration, which has the advantage that a wealth of algorithms are already available, the framework has been thoroughly tested, and comparison with the performance of a currently operational observatory is possible. The full simulation chain consists of four individual sequential steps, each of them producing a data product.

2.1 Air shower simulation

The first step is the generation of a library of air shower simulations for which we use CORSIKA [1] (v7.74, configured with UrQMD [2] for the low-energy hadronic interactions and QGSJetII-04 [3] for the high-energy hadronic interactions). The library consists of large sets of gamma-ray and proton showers, these are simulated on a E^{-2} spectrum from 30 GeV to 1 PeV (10 PeV for protons), and their directions are distributed isotropically up to a zenith angle of 65°. The geomagnetic field has been set to the current value of the magnetic field at lat/lon 18°S/70°W which is roughly in the middle of the range of locations that are considered for the observatory. For each air shower, the particles are saved at 8 observation levels between 4100 m and 5200 m, which spans the range of elevations of potential site candidates (see contribution [4]). With the same setup, smaller sets of primary helium, nitrogen, and iron nuclei have been simulated to evaluate science cases related to cosmic-ray composition.

---

[1]www.swgo.org
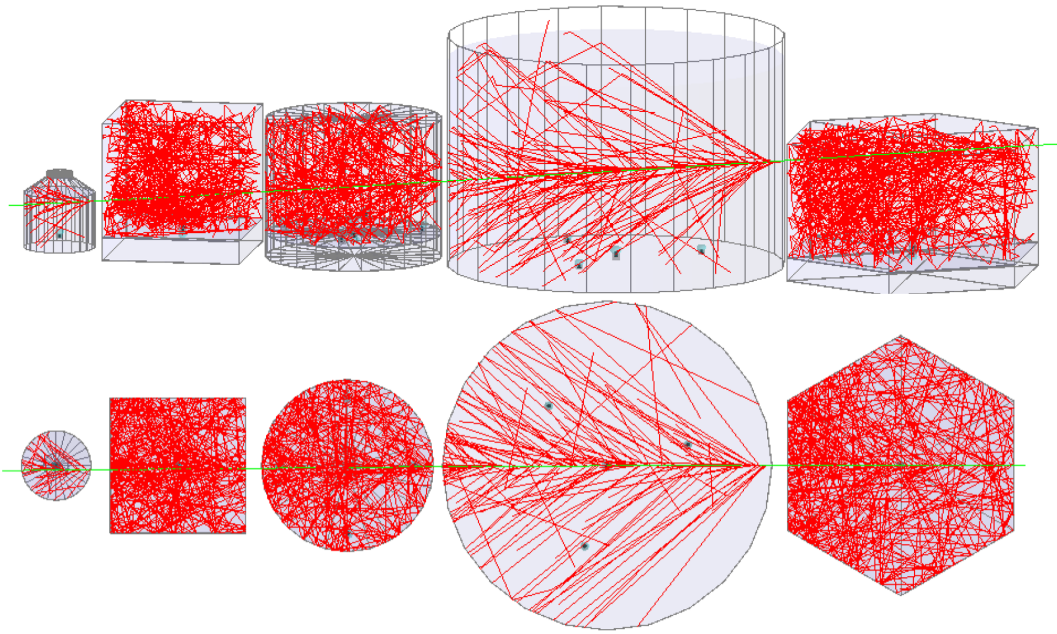
Figure 1: A nearly horizontal muon (green line) passing through the different tank shapes available in the detector simulation (side and top view). The red lines show a small fraction of the Cherenkov photon tracks. The smallest and largest cylindrical tanks have poorly reflective linings while the other tanks have highly reflective linings.

2.2 Detector response

The interactions of air shower particles with the detector are simulated using a model implemented in GEANT4[5]. The information of each Cherenkov photon generated by the relativistic charged particles in the water is collected at the impact point on the photo sensor. This part of the simulation chain is the most computing intensive, therefore several strategies are developed to make calculation of the detector response more efficient.

Firstly, by taking into account the wavelength dependent photon detection efficiency at the moment that photons are generated, we reduce the number of photons that need to be tracked and therefore reduce the calculation time. Secondly, for each photon arriving at the photo sensor, we store its impact point, direction, energy and the number of reflections it underwent. This information can be used to simulate several component options at once. By using the output of simulations with large high-efficiency photo sensors, smaller and/or less efficient sensors can be simulated by rejecting photons based on the stored information at a later stage. Similarly, by using a reflective lining around the water-volume in the initial simulation, non reflective linings can be simulated by rejecting photons that have non-zero values for the reflection counter.

The detector simulation is configurable by text-based steering cards. The shape, dimensions, materials of the detector unit can be chosen. Also the type of photo sensors and their number and locations within a detection unit can be set. In addition, the array layout is set up with an external steering card.

As an illustration of the flexibility of the detector simulations, we show in Figure 1 a muon passing through the different tank shape options we have currently available (see also [6]).

2.3 Event Reconstruction

The event reconstruction chain consists of several parts. The list of photons that are expected to generate a signal in a photo sensor are processed further. The electronics and the data acquisition are modeled and applied. This includes the superposition of noise, the response and processing of the electronics and the application of trigger conditions. For each electronics channel, signal amplitude and time are derived and they are sequentially used in the event reconstruction and classification. After event geometry and energy has been reconstructed, parameters are derived to estimate the type of the primary cosmic particle, mainly focusing on separating the electromagnetic cascades produced by primary gamma-rays (and electrons) from hardonic cascades initiated by cosmic-ray nuclei. After this step, event-lists are written out. The level of detail written to file per event can be set to single valued parameters per event or be extended to include the time and amplitude estimates of each channel. Currently, the event reconstruction chain is being developed and optimised.

2.4 Instrument Response Functions

The event-list parameters from the reconstruction chain, together with the information about how the air showers were distributed are used to build the Instrument Response Functions. The initial effort that started this work is focusing on making this part of the framework compatible with the standards in the field [7, 8]. This should allow for straightforward testing of science cases, where the end user can provide scripts that are similar to the ones being used for the Cherenkov Telescope Array or Fermi-LAT studies.

3. Strategy

3.1 A starting point

To get an initial starting point in the optimisation procedure for SWGO, we defined a reference design. The design parameters are chosen such that it should be a reasonably performing detector, but no serious optimisation steps have been taken yet. For all the individual components of this reference design a best estimate for the costs is currently being derived such that we can get a total cost estimate for a full observatory. The reference design consists of a dense inner array with a fill factor of roughly 80% and radius of 160 m. This array is surrounded by a less dense array with an outer radius of 300 m and a fill factor of about 5% (see Figure 2). The units in the inner and outer array are identical and the total number of detector units is 6600. The individual units correspond to a two compartment cylindrical tank with a diametre of 3.8 m (see Figure 1 third tank from the left). Each compartment contains a R5912-100 8" Photon Multiplier Tube from Hamamastsu and the height of the lower compartment is 0.5 m, while the height of the top compartment is 2.5 m. All inner surfaces are reflective (using white Tyvek), except the floor and ceiling in the upper compartment (black Polyproplene). Figure 2 shows the array layout and the response to two gamma-rays of different energies. This reference design will be used to develop and validate the end-to-end simulation framework and produce an initial set of IRFs which will be used to evaluate the science benchmarks [9].
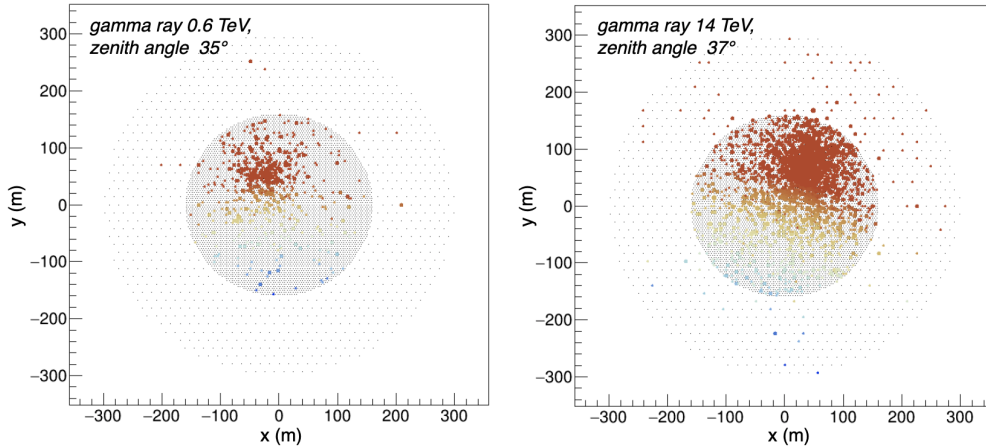
Figure 2: Reference array configuration with the response to two simulated gamma rays. Marker sizes give an indication of the signal amplitude and the colour coding shows the timing gradient (time increasing from blue to red).

3.2 Optimising

In the next step, the total cost of the reference design will be used as a constraint on other designs. By generating a cost model database for individual components, other detector design and layout options will be studied with the total price fixed. Each layout will be confronted with the science benchmarks in order to get an overview of the impact of design choices on the science potential of the observatory. The cost constraint in this approach is used to guide the design choices, the final design will depend on the total budget available for the construction and operation of the observatory. The phase space that we intend to explore in this way is indicated on the differential-point-source-sensitivity plot in Figure 3. As a conservative upper limit in the performance we picked the straw man design that was used in an earlier science case study[13]. This curve is obtained by scaling from the 2017 published HAWC performance to an array layout that is close to the reference design (Figure 2). We scaled the array layout, but not the intrinsic performance of the detector units with respect to HAWC detector units. The shaded region in Figure 3 is to indicate where different design options might enhance the sensitivity over the performance of the straw man design. We identified three energy regimes where improvements might be achieved with particular design choices.

Several design options under investigation aim to improve the low-energy performance with respect to the HAWC and LHAASO designs. Among these, are the lowering of the individual unit threshold and the possibility for sites at a higher elevation. The region in Figure 3 is indicative of a boost in performance, but the actual performance should become more clear when the design options are confronted with the specific science benchmark cases where low-energy performance is crucial, like the detection possibilities of gamma-ray bursts.

In the mid-energy range, preliminary studies indicate that significant improvements can be made on both the angular resolution and the background rejection [14–16]. Especially under investigations are compact units with dedicated muon tagging capabilities. To indicate a scale that
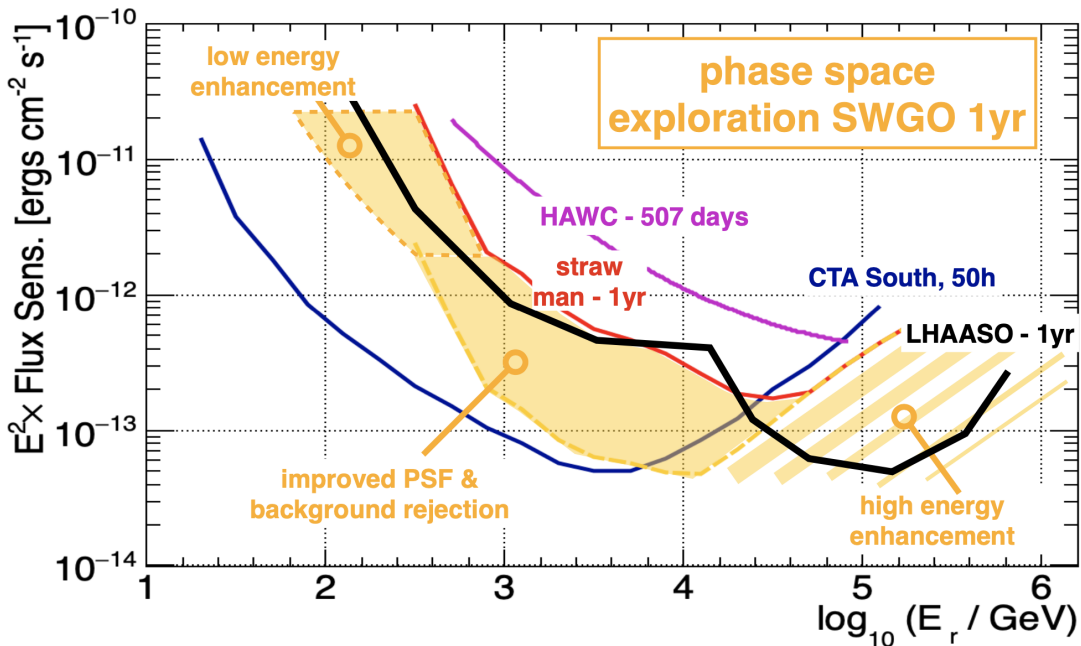
Figure 3: Differential point source sensitivity of several experiments[10–13] and the phase-space that will be explored in the design studies for SWGO (see text for more detail).

might be achievable, we applied scaling factors of 0.3 to the point spread function (PSF) and 10 to the background rejection efficiency of the straw man design as a lower-limit of the phase-space exploration.

The recent results from LHAASO show that a square kilometre array with a 10^{-5} background efficiency is feasible and that there are quite a few sources in the 0.1 - 1 PeV energy range [17]. This motivates us to investigate the options for enhancing the high-energy performance of SWGO by implementing a large (low density) outer array with good background rejection efficiency.

The outcome of the presented optimisation strategy will be used in the final design optimisation, which takes into account the constraints and exact properties of the proposed site of the observatory, as well as the decisions made on detector hardware implementation [18, 19].

Acknowledgements

References

[1] D. Heck et al., CORSIKA: A Monte Carlo Code to Simulate Extensive Air Showers (Forschungszentrum Karlsruhe GmbH, Karlsruhe, 1998)

[2] S. Bass et al., Microscopic models for ultra-relativistic heavy ion collisions. Prog. Part. Nucl. Phys. **41**, 255–369 (1998)

6

[3] S. Ostapchenko, Monte Carlo treatment of hadronic interactions in enhanced Pomeron scheme: QGSJET-II model. Phys. Rev. D **83**, 014018 (2011).

[4] M. Doro et al., PoS(ICRC2021)689

[5] S. Agostinelli et al.,Geant4 - A Simulation Toolkit, Nucl. Instrum. Meth. A **506** (2003) 250-303

[6] F. Bisconti et al., PoS(ICRC2021)895

[7] https://gamma-astro-data-formats.readthedocs.io/en/latest/

[8] L. Olivera-Nieto et al., PoS(ICRC2021)272

[9] U. Barres de Almeida et al., PoS(ICRC2021)893

[10] Vernetto, S. (2016). Journal of Physics: Con Series. **718**. 052043.

[11] https://www.cta-observatory.org/science/cta-performance

[12] A. U. Abeysekara et al., 2017 ApJ **843** 39

[13] A. Albert et al., 2019, arXiv:1902.08429

[14] W. Hofmann, On angular resolution limits for air shower arrays, Astroparticle Physics,**123**, 2020, 102479

[15] S. Kunwar et al, PoS(ICRC2021)902

[16] R. Conceição et al, PoS(ICRC2021)707

[17] Z. Cao et al, Ultrahigh-energy photons up to 1.4 petaelectronvolts from 12 gamma-ray Galactic sources, Nature, **594**, pages 33–36 (2021)

[18] J. Hinton et al., PoS(ICRC2021)023

[19] H. Goksu et al., PoS(ICRC2021)708

[20] F. Werner et al., PoS(ICRC2021)714

PoS(ICRC2021)903

Full Authors List: SWGO Collaboration

P. Abreu[1], A. Albert[2], E. O. Angüner[3], C. Arcaro[4], L. H. Arnaldi[5], J. C. Arteaga-Velázquez[6], P. Assis[1], A. Bakalová[7], U. Barres de Almeida[8], I. Batković[4], J. Bellido[9], E. Belmont-Moreno[10], F. Bisconti[11], A. Blanco[1], M. Bohacova[7], E. Bottacini[4], T. Bretz[12], C. Brisbois[13], P. Brogueira[1], A. M. Brown[14], T. Bulik[15], K. S. Caballero Mora[16], S. M. Campos[17] A. Chiavassa[11], L. Chytka[7], R. Conceição[1], G. Consolati[18], J. Cotzomi Paleta[19], S. Dasso[20], A. De Angelis[4], C. R. De Bom[8], E. de la Fuente[21], V. de Souza[22], D. Depaoli[11], G. Di Sciascio[23], C. O. Dib[24], D. Dorner[25], M. Doro[4], M. Du Vernois[26], T. Ergin[27], K. L. Fan[13], N. Fraija[8], S. Funk[28], J. I. García[17], J. A. García-González[29], S. T. García Roca[9], G. Giacinti[30], H. Goksu[30], B. S. González[1], F. Guarino[31], A. Guillén[32], F. Haist[30], P. M. Hansen[33], J. P. Harding[2], J. Hinton[30], W. Hofmann[30], B. Hona[34], D. Hoyos[17], P. Huentemeyer[35], F. Hueyotl-Zahuantitla[16] A. Insolia[36], P. Janecek[7], V. Joshi[28], B. Khelifi[37], S. Kunwar[30], G. La Mura[1], J. Lapington[38], M. R. Laspiur[17], F. Leitl[28], F. Longo[39], L. Lopes[1], R. Lopez-Coto[4], D. Mandat[7], A. G. Mariazzi[33], M. Mariotti[4], A. Marques Moraes[8], J. Martínez-Castro[40], H. Martínez-Huerta[41], S. May[42], D. G. Melo[43], L. F. Mendes[1], L. M. Mendes[1], T. Mineeva[24], A. Mitchell[44], S. Mohan[35], O. G. Morales Olivares[16], E. Moreno-Barbosa[19], L. Nellen[45], V. Novotny[7], L. Olivera-Nieto[30], E. Orlando[39], M. Pech[7], A. Pichel[20], M. Pimenta[1], M. Portes de Albuquerque[8], E. Prandini[4], M. S. Rado Cuchills[9], A. Reisenegger[46], B. Reville[30], C. D. Rho[47], A. C. Rovero[20], E. Ruiz-Velasco[30], G. A. Salazar[17], A. Sandoval[10], M. Santander[42], H. Schoorlemmer[30], F. Schüssler[48], V. H. Serrano[17], R. C. Shellard[8], A. Sinha[49], A. J. Smith[13], P. Surajbali[30], B. Tomé[1], I. Torres Aguilar[50], C. van Eldik[28], I. D. Vergara-Quispe[33], A. Viana[22], J. Vícha[7], C. F. Vigorito[11], X. Wang[35], F. Werner[30], R. White[30], M. A. Zamalloa Jara[9]

[1] Laboratório de Instrumentação e Física Experimental de Partículas (LIP), Av. Prof. Gama Pinto 2, 1649-003 Lisboa, Portugal

[2] Physics Division, Los Alamos National Laboratory, P.O. Box 1663, Los Alamos, NM 87545, United States

[3] Aix Marseille Univ, CNRS/IN2P3, CPPM, 163 avenue de Luminy - Case 902, 13288 Marseille cedex 09, France

[4] University of Padova, Department of Physics and Astronomy & INFN Padova, Via Marzolo 8 - 35131 Padova, Italy

[5] Centro Atómico Bariloche, Comisión Nacional de Energía Atómica, S. C. de Bariloche (8400), RN, Argentina

[6] Universidad Michoacana de San Nicolás de Hidalgo, Calle de Santiago Tapia 403, Centro, 58000 Morelia, Mich., México

[7] FZU, Institute of Physics of the Czech Academy of Sciences, Na Slovance 1999/2, 182 00 Praha 8, Czech Republic

[8] Centro Brasileiro de Pesquisas Físicas, R. Dr. Xavier Sigaud, 150 - Rio de Janeiro - RJ, 22290-180, Brazil

[9] Academic Department of Physics – Faculty of Sciences – Universidad Nacional de San Antonio Abad del Cusco (UNSAAC), Av. de la Cultura, 733, Pabellón C-358, Cusco, Peru

[10] Instituto de Física, Universidad Nacional Autónoma de México, Sendero Bicipuma, C.U., Coyoacán, 04510 Ciudad de México, CDMX, México

[11] Dipartimento di Fisica, Università degli Studi di Torino, Via Pietro Giuria 1, 10125, Torino, Italy

[12] RWTH Aachen University, Physics Institute 3, Otto-Blumenthal-Straße, 52074 Aachen, Germany

[13] University of Maryland, College Park, MD 20742, United States

[14] Durham University, Stockton Road, Durham, DH1 3LE, United Kingdom

[15] Astronomical Observatory, University of Warsaw, Aleje Ujazdowskie 4, 00478 Warsaw, Poland

[16] Facultad de Ciencias en Física y Matemáticas UNACH, Boulevard Belisario Domínguez, Km. 1081, Sin Número, Terán, Tuxtla Gutiérrez, Chiapas, México

[17] Facultad de Ciencias Exactas, Universidad Nacional de Salta, Avda. Bolivia N° 5150, (4400) Salta Capital, Argentina

[18] Department of Aerospace Science and Technology, Politecnico di Milano, Via Privata Giuseppe La Masa, 34, 20156 Milano MI, Italy

[19] Facultad de Ciencias Físico Matemáticas, Benemérita Universidad Autónoma de Puebla, C.P. 72592, México

[20] Instituto de Astronomia y Fisica del Espacio (IAFE, CONICET-UBA), Casilla de Correo 67 - Suc. 28 (C1428ZAA), Ciudad Autónoma de Buenos Aires, Argentina

[21] Universidad de Guadalajara, Blvd. Gral. Marcelino García Barragán 1421, Olímpica, 44430 Guadalajara, Jal., México

[22] Instituto de Física de São Carlos, Universidade de São Paulo, Avenida Trabalhador São-carlense, nº 400, Parque Arnold Schimidt - CEP 13566-590, São Carlos - São Paulo - Brasil

[23] INFN - Roma Tor Vergata and INAF-IAPS, Via del Fosso del Cavaliere, 100, 00133 Roma RM, Italy

[24] Dept. of Physics and CCTVal, Universidad Tecnica Federico Santa Maria, Avenida España 1680, Valparaíso, Chile

[25] Universität Würzburg, Institut für Theoretische Physik und Astrophysik, Emil-Fischer-Str. 31, 97074 Würzburg, Germany

[26] Department of Physics, and the Wisconsin IceCube Particle Astrophysics Center (WIPAC), University of Wisconsin, 222 West Washington Ave., Suite 500, Madison, WI 53703, United States

[27] TUBITAK Space Technologies Research Institute, ODTU Campus, 06800, Ankara, Turkey

[28] Friedrich-Alexander-Universität Erlangen-Nürnberg, Erlangen Centre for Astroparticle Physics, Erwin-Rommel-Str. 1, D 91058 Erlangen, Germany

[29] Tecnologico de Monterrey, Escuela de Ingeniería y Ciencias, Ave. Eugenio Garza Sada 2501, Monterrey, N.L., 64849, México

[30] Max-Planck-Institut für Kernphysik, P.O. Box 103980, D 69029 Heidelberg, Germany

[31] Università di Napoli "Federico II", Dipartimento di Fisica "Ettore Pancini", and INFN Napoli, Complesso Universitario di Monte Sant'Angelo - Via Cinthia, 21 - 80126 - Napoli, Italy

[32] University of Granada, Campus Universitario de Cartuja, Calle Prof. Vicente Callao, 3, 18011 Granada, Spain

PoS(ICRC2021)903

[33] IFLP, Universidad Nacional de La Plata and CONICET, Diagonal 113, Casco Urbano, B1900 La Plata, Provincia de Buenos Aires, Argentina

[34] University of Utah, 201 Presidents' Cir, Salt Lake City, UT 84112, United States

[35] Michigan Technological University, 1400 Townsend Drive, Houghton, MI 49931, United States

[36] Dipartimento di Fisica e Astronomia "E. Majorana", Catania University and INFN, Catania, Italy

[37] APC–IN2P3/CNRS, Université de Paris, Bâtiment Condorcet, 10 rue A.Domon et Léonie Duquet, 75205 PARIS CEDEX 13, France

[38] University of Leicester, University Road, Leicester LE1 7RH, United Kingdom

[39] Department of Physics, University of Trieste and INFN Trieste, via Valerio 2, I-34127, Trieste, Italy

[40] Centro de Investigación en Computación, Instituto Politécnico Nacional, Av. Juan de Dios Bátiz S/N, Nueva Industrial Vallejo, Gustavo A. Madero, 07738 Ciudad de México, CDMX, México

[41] Department of Physics and Mathematics, Universidad de Monterrey, Av. Morones Prieto 4500, San Pedro Garza García 66238, N.L., México

[42] Department of Physics and Astronomy, University of Alabama, Gallalee Hall, Tuscaloosa, AL 35401, United States

[43] Instituto de Tecnologías en Detección y Astropartículas (CNEA-CONICET-UNSAM), Av. Gral Paz 1499 - San Martín - Pcia. de Buenos Aires, Argentina

[44] Department of Physics, ETH Zurich, CH-8093 Zurich, Switzerland

[45] Instituto de Ciencias Nucleares, Universidad Nacional Autónoma de México (ICN-UNAM), Cto. Exterior S/N, C.U., Coyoacán, 04510 Ciudad de México, CDMX, México

[46] Departamento de Física, Facultad de Ciencias Básicas, Universidad Metropolitana de Ciencias de la Educación, Av. José Pedro Alessandri 774, Ñuñoa, Santiago, Chile

[47] Department of Physics, University of Seoul, 163 Seoulsiripdaero, Dongdaemun-gu, Seoul 02504, Republic of Korea

[48] Institut de recherche sur les lois fondamentales de l'Univers (IRFU), CEA, Université Paris-Saclay, F-91191 Gif-sur-Yvette, France

[49] Laboratoire Univers et Particules de Montpellier, CNRS, Université de Montpelleir, F-34090 Montpellier, France

[50] Instituto Nacional de Astrofísica, Óptica y Electrónica (INAOE), Luis Enrique Erro 1, Puebla, México

PoS(ICRC2021)903